Conjugate Additions of 1-Propenylphosphonates to Metalated Schöllkopf's Bis-lactim Ether: Stereocontrolled Access to 2-Amino-3-methyl-4-phosphonobutanoic Acids

Vicente Ojea,*,† María Ruiz,† Gideon Shapiro, and Esteban Pombo-Villar*

Preclinical Research, Novartis Pharma Ltd., CH-4002 Basel, Switzerland

Received September 7, 1999

Diastereoselectivity in the conjugate addition of metalated Schöllkopf's bis-lactim ethers **5a**−**e** to (*E*)- and (*Z*)-1-propenylphosphonates **4a**,**b** was studied experimentally and theoretically and utilized to achieve a direct and stereocontrolled synthesis of all four diastereoisomers of 2-amino-3-methyl-4-phosphonobutanoic acid, **6a**,**b** and their enantiomers. The relative stereochemistry was assigned from an NMR study of cyclic derivatives **13a**,**b**. According to semiempirical calculations, both in vacuo (PM3) or a dielectric continuum (PM3/COSMO), initial lithium−phosphoryl coordination, without an energy barrier, to form a solvated chelate complex is followed by the rate-determining reorganization to the 1,4-addition product through an eight-membered transition state. The translation of the *Z*,*E* geometry into a syn,anti configuration at the adducts originates from an orientational preference in the transition state for a *compact* disposition of the reaction partners.

Introduction

L-Glutamic acid mediates fast excitatory transmission at the majority of central nervous system synapses and also participates in neuronal plasticity and neurotoxicity.[1] Synaptically released glutamate exerts its effects via activation of ligand-gated cation channels (the ionotropic glutamate receptors) and metabotropic glutamate receptors (mGluRs), which modulate intracellular second messengers through G protein-coupled processes. Glutamate receptors have attracted considerable attention because of their therapeutic potential for the treatment of a range of chronic and acute CNS disorders with social significance, such as stroke, epilepsy, and Alzheimer's disease.[2] To date, mGluRs have been distinguished into three groups, based on sequence homology, signal transduction mechanisms, and agonist pharmacology. In particular, receptors of group III (subtypes mGluR4 and mGluR6−8) are characterized by their selective response to several phosphonic acid derivatives. Thus, they are selectively activated by L-2-amino-4-phosphonobutanoic acid (L-AP4, **1**, see Chart 1) and competitively antagonized by the α-methylated derivatives of L-AP4 (MAP4, **2**) and 4-phosphonophenylglycine (MPPG, **3**).[3] Biological research on mGluRs function awaits the development of more potent and selective agonist and antagonists, to clearly define the potential of these receptors as drug targets. As the molecular basis for the glutamate recognition and binding at the mGluRs proteins has not been elucidated yet, the development of high-affinity ligands still relies on structural modification of established structures and screening of new lead compounds. As part of a project directed toward the design of new bioactive phosphonates,[4] we report now the diastereoselective synthesis of all four diastereoisomers of 2-amino-3-methyl-4-phosphonobutanoic acid, prepared in order to study the stereochemical requirements for a potent binding at group III of mGluRs.[5]

Chart 1. Agonist and Antagonists of the mGluRs of Group III

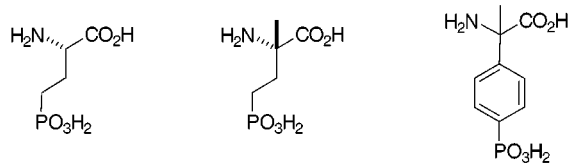

L-AP4 (**1**) MAP4 (**2**) MPPG (**3**)

Although the additions of organometallic reagents to electron-deficient alkenes constitute an important and well-known method in asymmetric synthesis,[6] and unsaturated systems bearing phosphonate groups act as acceptors with a variety of nucleophiles,[7] few examples can be found in the literature for stereoselective additions to alkenylphosphonates.[8] For the synthesis of nonproteinogenic amino acids, conjugate additions of metalated Schöllkopf's bis-lactim ethers to several unsaturated systems have been shown as a valuable protocol that enables reasonably high levels of stereocontrol at both α and β positions.[9] These precedents

† Current address: Departamento de Química Fundamental e Industrial, Facultade de Ciencias, Universidade da Coruña. Campus A Zapateira s/n, 15071 A Coruña, Spain. E-mail: ojea@udc.es.

(1) *CNS Neurotransmitters and Neuromodulators: Glutamate*; Stone, T. W., Ed.; CRC: Boca Raton, FL, 1995.

(2) (a) Knöpfel, T.; Gasparini, F. *Drug Discovery Today* **1996**, *1*, 103. (b) Knöpfel, T.; Kuhn, R.; Allgeier, H. *J. Med. Chem.* **1995**, *38*, 1417.

(3) Jane, D. E.; Pittaway, K.; Sunter, D. C.; Thomas, N. K.; Watkins, J. C. *Neuropharmacology* **1995**, *34*, 851. (b) Jane, D. E.; Jones, P. L. St. J.; Pook, P. C.-K.; Tse, H.-W.; Watkins, J. C. *Br. J. Pharmacol.* **1994**, *112*, 809.

(4) Ojea, V.; Conde, S.; Ruiz, M.; Fernández, M. C.; Quintela, J. M. *Tetrahedron Lett.* **1997**, *38*, 4311 and references therein.

(5) Part of this work was already presented as preliminary communications: (a) Ojea, V.; Ruiz, M.; Vilar, J.; Quintela, J. M. *Tetrahedron*: *Asymmetry* **1996**, *7*, 3335. (b) Ojea, V.; Ruiz, M.; Shapiro, G.; Pombo-Villar, E. *Tetrahedron Lett.* **1994**, *35*, 3273.

(6) Perlmutter, P. In *Conjugate Addition Reactions in Organic Synthesis*; Baldwin, J. E., Magnus, P. D., Eds.; Organic Chemistry Series, Vol. 9; Pergamon: Oxford, 1992.

(7) (a) Afarinkia, K.; Binch, H. M.; Modi, C. *Tetrahedron Lett.* **1998**, *39*, 7419. (b) Baldwin, I. C.; Beckett, R. P.; Williams, J. M. J. *Synthesis* **1996**, 34. (c) Zindel, J.; Meijere, A. *Synthesis* **1994**, 190. (d) Minami, T.; Motoyoshiya, J. *Synthesis* **1992**, 333 and references therein. (e) Darling, S. D.; Muralidharan, F. N.; Muralidharan, V. B. *Tetrahedron Lett.* **1979**, *30*, 2757 and 2761. See also references cited in ref 5b.

10.1021/jo991402w CCC: $19.00
Published on Web 03/04/2000

Scheme 1. Stereocontrolled Synthesis of L-AP4 Derivatives

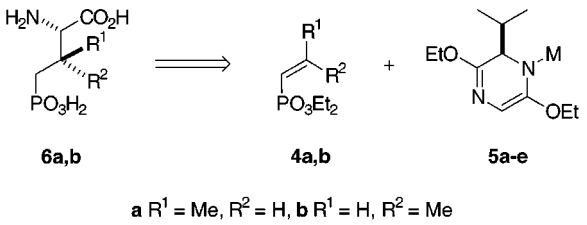

6a,b **4a,b** **5a-e**

a R^1 = Me, R^2 = H, **b** R^1 = H, R^2 = Me

Scheme 2. Preparation of 1-Propenylphosphonates 4a,b

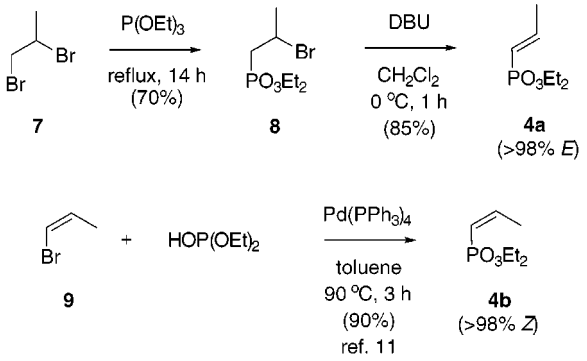

prompted us to explore the conjugate additions of metalated bis-lactim ethers to alkenylphosphonates, as a new approach to 2-amino-4-phosphonobutanoic acids. In this paper, we wish to report our results on the face-selective conjugate additions of metalated bis-lactim ethers **5a**−**e** to (*E*)- and (*Z*)-1-propenylphosphonates **4a**,**b** that allow a direct and stereocontrolled access to optically pure AP4 analogues **6a**,**b** (see Scheme 1). To gain more insight into the origin of the stereoselection in the addition process, and assess its scope and limitations in asymmetric synthesis, we have also carried out a theoretical analysis of the possible reaction mechanisms. Thus, a semiempirically optimized transition-state model that rationalizes the stereochemical outcome of the addition process is also put forward.

Experimental Results and Discussion

The preparation of the 1-propenylphosphonate esters **4a**,**b** was accomplished as depicted in Scheme 2. Although Arbuzov reaction of triethyl phosphite with 1 equiv of 1,2-dibromopropane (**7**) was reported to be completely unsuccessful,[10] 2-bromopropylphosphonate **8** could be obtained in good yield simply by using **7** in a large excess. Thus, after refluxing triethyl phosphite and 6 equiv of 1,2-dibromopropane for 14 h, phosphonate **8** was obtained (70% yield) together with *O*,*O*-diethylethylphosphonate as a side product (25%). Both compounds and unreacted 1,2-dibromopropane could be easily separated by distillation at reduced pressure. Dehydrobromination of **8** by treatment with DBU at 0 °C afforded the desired (*E*)-1-propenylphosphonate **4a** in good yield. (*Z*)-1-Propenylphosphonate **4b** was prepared directly and stereospecifically by Pd(0)-catalyzed coupling of commercial *cis*-1-bromo-1-propene (**9**) and diethyl phosphite, as described in the literature.[11] According to ^{31}P NMR analyses, propenylphosphonates **4a** and **4b** were obtained with >98% (*E*)- and (*Z*)-configuration, respectively.

1-Propenylphosphonates **4a** and **4b** underwent a highly stereoselective conjugate addition of lithiated Schöllkopf's bis-lactim ethers, in a fashion similar to that previously reported for α,β-unsaturated carboxylic acid esters.[9g] Slow addition of propenylphosphonates **4a** or **4b** to 1 equiv of **5a** at −78 °C in THF, followed by immediate acetic acid quenching and aqueous workup, gave mixtures of the desired adducts **10a** and **10b** in 33% combined yield, along with 1:2 addition products **11** (see Scheme 3). Integration of the ^{1}H-decoupled ^{31}P NMR spectra of the crude reaction mixtures revealed a very high asymmetric induction in the formation of both new chiral centers, as well as complementary stereochemical courses in the additions to both acceptors, only differing in the geometry of the double bond. After the isolation of the fractions containing the 1:1 addition products by flash chromatography, integration of the pairs of doublets corresponding to the isopropyl groups in the ^{1}H NMR spectra confirmed the formation of mixtures of adducts **10a**/**10b** with 96:4 and 4:96 ratios in the cases **a** and **b**, respectively. In this way, the diastereomeric excess of the 2,5-trans-2,1′-anti adduct **10a** in the addition to the (*E*)-1-propenylphosphonate **4a**, and of the 2,5-trans-2,1′-syn adduct **10b** in the addition to (*Z*)-1-propenylphosphonate **4b**, were both higher than 90%. Evidence supporting the relative configuration on adducts was obtained by NMR analyses. Thus, for **10b**, the H-5 resonance appears at 3.89 ppm, as a triplet with $^5J_{H2H5}$ = 3.5 Hz, typical for a trans relation of substituents at the pyrazine ring.[9e,f] The relative configurations at position 1′ were assigned on the basis of the sets of NOEs observed for cyclic derivatives of **10a**,**b**, as will be described below. Absolute configurations follow from the use of bis-lactim ethers derived from D-Val, as there is ample precedent.[9]

Having shown the feasibility of synthesizing both anti and syn adducts **10a**,**b**, the influence of additives and reaction conditions on the yield and stereoselection of the conjugate addition was examined, the most salient results being summarized in Table 1. While addition of 12-crown-4 to the lithium azaenolate **5a** prior to reaction with acceptor **4a** had no appreciable effect on the process, in the presence of an excess of HMPA the same addition proceeded with very low diastereoselectivity, giving rise to a 2.1:1.0:0.9:0.5 mixture of all four possible stereoisomers (see Table 1, entries 3 and 4). Thus, the disruptive role of lithium solvation by HMPA highlights the importance of ordered lithium-chelated aggregates in the stereochemical course of the addition process. Conversely, the 12-crown-4 may simply replace solvent molecules in its coordination to lithium, without modification of the

(8) (a) Enders, D.; Wahl, H.; Papadopoulos, K. *Tetrahedron* **1997**, *53*, 12961 and references therein. (b) Groth, U.; Richter, L.; Schöllkopf, U. *Tetrahedron* **1992**, *48*, 117. (c) Bodalski, R.; Michalski, T.; Monkiewicz, J.; Pietrusiewicz, K. Addition of Lithium Dialkylcuprates to α,β-Unsaturated Phosphoryl Compounds. In *Phosphorus Chemistry*; Comstock, M. J., Ed.; ACS Symposium Series 171; American Chemical Society: Washington, DC, 1981; p 245.

(9) (a) Williams, R. M. *Synthesis of Optically Active α-Amino Acids;* Baldwin, J. E., Magnus, P. D., Eds.; Organic Chemistry Series, Vol. 7; Pergamon: Oxford, 1989. (b) Schöllkopf, U.; Pettig, D.; Schulze, E.; Klinge, M.; Egert, E.; Benecke, B.; Noltemeyer, M. *Angew. Chem., Int. Ed. Engl.* **1988**, *27*, 1194. (c) Pettig, D.; Schöllkopf, U. *Synthesis* **1988**, 173. (d) Schöllkopf, U.; Schröder, J. *Liebigs Ann. Chem.* **1988**, *87*. (e) Schöllkopf, U.; Kühnle, W.; Egert, E.; Dyrbusch, M. *Angew. Chem., Int. Ed. Engl.* **1987**, *26*, 480. (f) Hartwig, W.; Born, L. *J. Org. Chem.* **1987**, *52*, 4352. (g) Schöllkopf, U.; Pettig, D.; Busse, U.; Egert, E.; Dyrbusch, M. *Synthesis* **1986**, 737.

(10) Ford-Moore, A. H.; Howarth Williams, J. *J. Chem. Soc.* **1947**, 1465.

(11) Hirao, T.; Masunaga, T.; Yamada, N.; Ohshiro, Y.; Agawa, T. *Bull. Chem. Soc. Jpn.* **1982**, *55*, 909.

Scheme 3. Conjugate Addition of 1-Propenylphosphonates 4a,b to Metalated Bis-lactim Ethers 5a−e

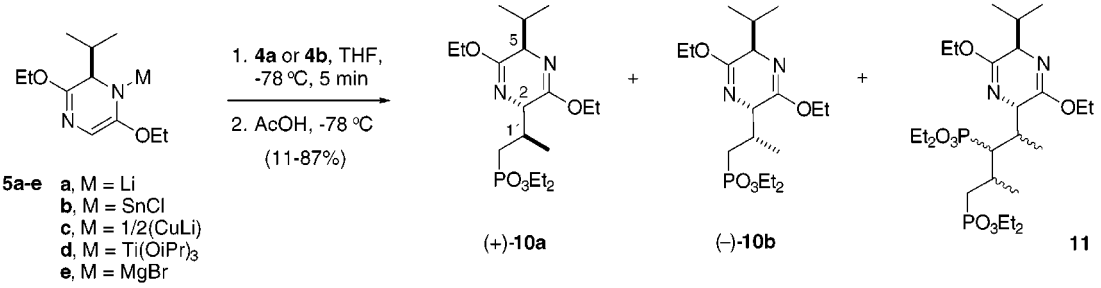

Table 1. Conjugate Additions of Metalated Bis-lactim Ethers 5a−e to 1-Propenylphosphonates 4a,b

entry	5a	4a	4b	8	additive (equiv)	yield[a] (%)	10a:10b ratio[b]
1	1	1				33	23:1
2	1		1			33	1:25
3	1	1			12-crown-4 (2)	29	20:1
4	1	1			HMPA (10)	27	1:2.1
5	1	1			$SnCl_2$ (1)	NR	
6	1	1			$CuBr_2 \cdot SMe_2$ (1)	NR	
7	1	1			$TiCl(OiPr)_3$ (1)	26	13:1
8	1	1			$MgBr_2 \cdot OEt_2$ (1)	11	40:1
9	2	1				62	21:1
10	2		1			66	1:22
11	2	1			$MgBr_2 \cdot OEt_2$ (1)	27	40:1
12	3	1				87	23:1
13	3		1			85	1:24
14	1	0.10		0.90		48	18:1
15	1	0.33		0.66		60	19:1
16	1	0.50		0.50		50	19:1
17	2	0.33		0.66		87	19:1

[a] Isolated yield of mixtures of adducts **10a**/**10b**, after column chromatography. [b] Determined by integration of ^{31}P NMR spectra. NR = no reaction was observed.

chelation control in the process. Several reports from different groups have shown a strong increase in the diastereoselectivity of aldol and conjugate additions of metalated Schöllkopf's bis-lactim ethers when the lithium atom is exchanged by Sn(II),[12] Cu(I),[9d] or Ti(IV).[13] On the basis of these precedents, azaenolate **5a** was allowed to react, in THF at low temperature, with stoichiometric amounts of $SnCl_2$, $CuBr_2 \cdot SMe_2$, $ClTi(O^iPr)_3$, or $MgBr_2 \cdot OEt_2$, to produce the corresponding transmetalated azaenolates **5b**−**e**,[14] prior to the addition of the alkenylphosphonate **4a**. No reaction was observed for the tin(II) and copper(I) azaenolates (**5b** and **5c**, respectively) under the standard conditions (−78 °C, THF, 5 min) or with longer reaction times and warming (up to 10 h and 0 °C, see Table 1, entries 5 and 6). Reactions of **4a** with the titanium and magnesium azaenolates were complete at low temperature in a few minutes but gave the mixtures of adducts **10a/10b** with lower yields. Switching the metal to Ti or Mg did not change the stereochemical course of the addition, but led to the anti adducts with a slightly different selectivity. Thus, the anti/syn ratio decreased to 13:1 by using the titanium azaenolate, whereas a remarkable 40:1 ratio was observed in the presence of magnesium (see Table 1, entries 7 and 8).

We reasoned that the chemical yield of 1:1 addition products was lowered by further addition of the initially formed adduct anion to the α,β-unsaturated acceptor. Thus, to reduce the dimerization process, we carried out the addition process using an excess of the azaenolate. By using 2 equiv of the lithium azaenolate **5a**, the yields of the mixtures of 1:1 adducts resulting from the addition to either **4a** or **4b** were increased to 62 or 66%, respectively. In the presence of magnesium, the same conditions led to **10a**/**10b** with 27% yield (see Table 1, entries 9−11). The mixtures of adducts **10a**,**b** could be isolated with yields higher than 85% when 3 equiv of lithium azaenolate was used (see Table 1, entries 12 and 13). On the basis of our previous studies on the conjugate addition to vinylphosphonates,[15] it was expected that the initial anionic adduct would be effective in producing the alkenylphosphonate **4a** in situ, via dehydrohalogenation of the 2-bromopropylphosphonate **8**, thus suppressing oligomerization. When mixtures of **4a**/**8** were added to the lithium azaenolate, the anti adduct was obtained with improved yields and with high diastereoselectivity (see Table 1, entries 14−17). In this manner, using 1 equiv of a mixture of **4a** and **8** in a 1:2 ratio and 2 equiv of **5a**, a mixture of 1:1 adducts containing **10a** with 90% diastereomeric excess could be isolated in 87% yield. Apparently, the conjugate addition of lithium azaenolate to the alkenylphosphonate **4a** is faster than the elimination of **8**, and the initially formed phosphonate carbanion is more basic than the lithium azaenolate. In all cases, the excess of Schöllkopf's reagent could be recovered and showed no racemization.[16]

The separation of **10a** from **10b** could be achieved by medium-pressure liquid chromatography to provide products of high purity, with a diastereomeric excess higher than 98%, on a multigram scale. Mild acid hydrolysis of the bis-lactim ether provided the aminoesters **12a** and **12b** in excellent yield after removal of the valine ester by chromatography (see Scheme 4). Vigorous acid hydrolysis of the amino esters allowed, after purification by reversed-phase chromatography, the isolation of the 2-amino-3-methyl-4-phosphonobutanoic acids (**6a** and **6b**) in excellent yields. Starting from the Schöllkopf's bis-lactim ether derived from L-valine, the corresponding enantiomers of **6a**,**b** were prepared in an analogous fashion.

Since none of the synthesized adducts, esters, or amino acids provided crystals suitable for an X-ray crystal structure determination, a cyclic derivative was sought that could enable the assignment of the relative configurations by ^1H NMR spectroscopy. The six-membered amino-oxaphosphorinane derivatives **13a**,**b** were attrac-

(12) (a) Ruiz, M.; Ojea, V.; Quintela, J. M. *Synlett* **1999**, 204. (b) Ruiz, M.; Ruanova, T. M.; Ojea, V.; Quintela, J. M. *Tetrahedron Lett.* **1999**, *40*, 2021. (c) Kobayashi, S.; Furuta, T.; Hayashi, T.; Nishijima, M.; Hanada, K. *J. Am. Chem. Soc.* **1998**, *120*, 908.

(13) (a) Schöllkopf, U.; Bardenhagen, J. *Liebigs Ann. Chem.* **1987**, 393. (b) Grauert, M.; Schöllkopf, U. *Liebigs Ann. Chem.* **1985**, 1817.

(14) Hünig, S.; Klaunzer, N.; Wenner, H. *Chem. Ber.* **1994**, *127*, 165.

(15) Shapiro, G.; Buechler, D.; Ojea, V.; Pombo-Villar, E.; Ruiz, M.; Weber, H. P. *Tetrahedron Lett.* **1993**, *34*, 6255.

(16) Multigram quantities of Schöllkopf's reagents were obtained from Novartis kilo laboratory.

Scheme 4

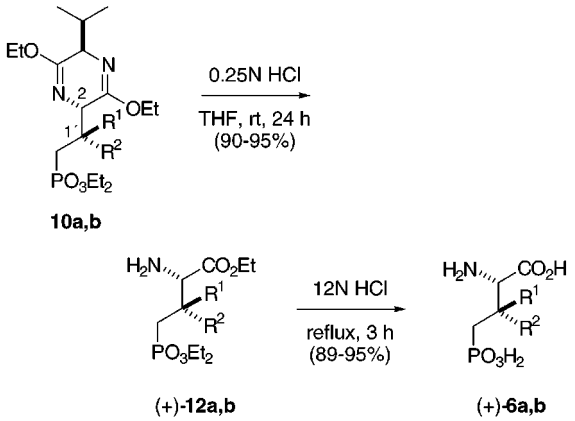

a R^1 = Me, R^2 = H, **b** R^1 = H, R^2 = Me

Scheme 5

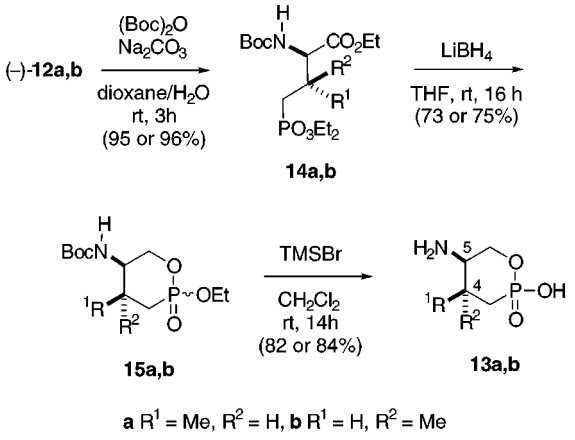

a R^1 = Me, R^2 = H, **b** R^1 = H, R^2 = Me

tive in this regard, because of the strong preference for the chair conformation reported for similarly 4-methyl-substituted systems (see Scheme 5).[17] Conversion of amino esters **12a**,**b** into such cyclic derivatives required the selective reduction of the carboxylic ester in the presence of the phosphonate group. Attempts to achieve this reduction with lithium aluminum hydride in THF resulted in complex mixtures of products, by simultaneous reduction of the phosphonic ester and epimerization at the α-center. Sodium borohydride in refluxing methanol caused transesterification of the carboxylic ester and epimerization of the α-center, while with calcium borohydride or DIBALH in THF there was no reaction. Chemoselective reduction of the carboxylic ester in the presence of the phosphonate was eventually achieved on the *N*-Boc derivatives of amino esters **14a**,**b**, employing lithium borohydride in anhydrous THF at room temperature. Moreover, under these conditions, cyclization of the reduction intermediates to afford the *N*-Boc-amino-oxaphosphorinane derivatives **15a**,**b** was observed. While **15a** was obtained as one single diastereoisomer, **15b** was isolated as a mixture of epimers at the phosphorus center in a 2.7:1 ratio, which could not be separated by chromatography. The conformational

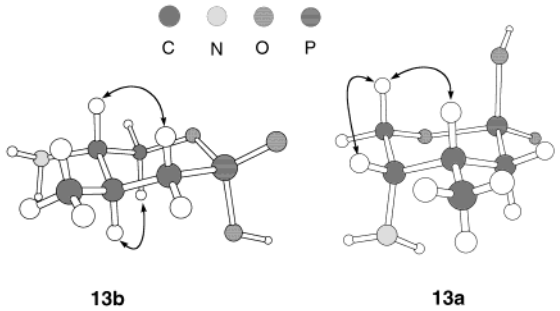

13b **13a**

Figure 1. PM3-optimized geometries for the cyclic derivatives **13a**,**b**, showing characteristic NOEs.

preferences of the substituents in a six-membered cyclic transition state with a bipyramidal phosphorus atom may account for this result, as was reported for the related specific ring opening of cyclic phosphonates by alkoxides.[18] The *N*-Boc and *O*-ethyl ester groups were cleaved with trimethylsilyl bromide in THF at room temperature to give **13a**,**b** as pure diastereoisomers.

A single chair conformation was observed for each compound **13a**,**b** in the ^{1}H NMR spectra (D_2O, 400 MHz, 25 °C). For compound **13b**, a doublet of triplets was observed for H-5 at $\delta = 3.24$ with coupling constants of 9.1 and 3.1 Hz. The major coupling constant indicated a diaxial relationship between H-5 and H-4, with a degenerate coupling of H-5 to H-6ax. Furthermore, the complete set of NOE cross-peaks that were observed by ^{1}H–^{1}H ROESY[19] was consistent with this trans-stereochemical assignment. The assignment of the cis configuration for diastereoisomer **13a** follows by elimination and is also consistent with the NOEs observed for that compound. The observed NOEs were supported by semiempirical calculations: the refined geometries in the gas phase for compounds **13a**,**b** were in agreement with the conformations in solution deduced from NMR spectroscopy, as depicted in Figure 1. All these results allow us to assume a 2,1′-anti configuration for adduct **10a** and a 2,1′-syn configuration for adduct **10b**.

The stereoselectivity of the conjugate addition to propenylphosphonates **4a** and **4b** is concordant with the stereochemical course reported for the additions of lithiated Schöllkopf's bis-lactim ether to 2-alkenoates[9e,f] and other (*E*)-alkenylphosphonates.[20] The stereochemical outcome of the process seems to be both reagent- and substrate-controlled. While the influence of the chiral glycine equivalent determines the absolute stereochemistry at the addition products, the relative configuration of the new chiral centers exclusively depends on the geometry of the propenylphosphonate. In this way, the reaction results in an almost complete translation of the *Z* or *E* geometry into a syn or anti configuration at the 1,4-addition products, as was previously observed with other conjugate additions to stereodefined enolates.[21]

Computational Results: PM3 Transition Structures and Energetics. On the basis of the experimental data, Heathcock and Oare have proposed that low-

(17) (a) Berkowitz, D. B.; Eggen, M.-J.; Shen, Q.; Shoemaker, R. K. *J. Org. Chem.* **1996**, *61*, 4666. (b) Bergesen, K.; Vikane, T. *Acta Chem. Scand.* **1972**, *26*, 1794. For the conformational preferences of other substituted 1,2-oxaphosphorinanes, see: Tasz, M. K.; Rodriguez, O. P.; Cremer, S. E.; Hussain, M. S.; Mazhar-ul-Haque *J. Chem. Soc., Perkin Trans. 2* **1996**, 2221, and references therein.

(18) (a) Thatcher, G. R. J.; Kluger, R. *Adv. Phys. Org. Chem.* **1989**, *25*, 99. (b) Hall, C. R.; Inch, T. D. *Tetrahedron* **1980**, *36*, 2059.

(19) Griesinger, C.; Ernst, R. R. *J. Magn. Reson.* **1987**, *75*, 261.

(20) Ojea, V.; Fernández, M. C.; Ruiz, M.; Quintela, J. M. *Tetrahedron Lett.* **1996**, *37*, 5801.

(21) For a review of the stereochemistry of the Michael addition reaction, see: (a) Leonard, J. *Contemp. Org. Synth.* **1994**, *1*, 387. (b) Oare, D. A.; Heathcock, C. H. *Top. Stereochem.* **1989**, *19*, 227.

Scheme 6. Reaction Pathway Proposed for the Addition of Lithiated Schöllkop's Bis-lactim Ether 16 to 1-Propenylphosphonates 17a,b

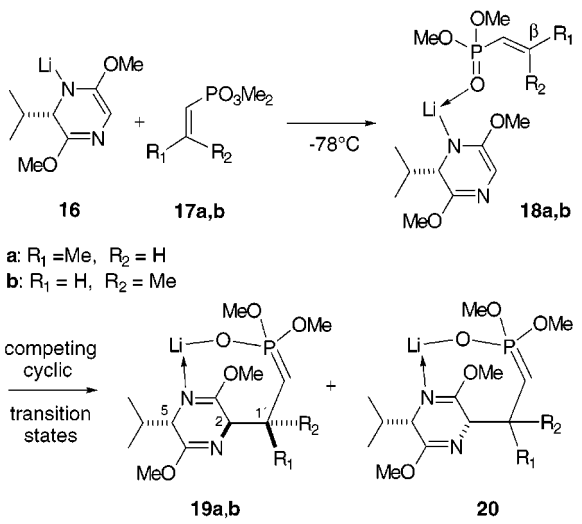

temperature enolate Michael additions to α,*β*-unsaturated carbonyl compounds are kinetically controlled. By analogy with the Zimmermann−Traxler model for aldol additions, these authors suggested that the stereochemical course of those processes can be rationalized by assuming the participation of cyclic, rate-determining transition structures.[22] Bernardi et al. have studied this hypothesis by ab initio methods and have verified that eight-membered transition structures account for the experimental results.[23] On the basis of these precedents, we have recently reported that competitive cyclic transition structures can be located on the MNDO and PM3 potential energy surfaces obtained for a minimal molecular prototype of the bis-lactim/alkenylphosphonate system. This competitive transition state model allowed a qualitative rationalization of the observed stereoselectivity trends for the conjugate addition.[5a] These results prompted us to evaluate the efficiency of such transition state model for the analysis of more realistic situations, considering full substitution of the reaction partners and also solvation effects. With this purpose we have carried out a theoretical study of the addition of the lithiated bis-lactim ether **16**, derived from *cyclo*-[L-Val-Gly], to *O*,*O*-dimethyl 1-propenylphosphonates **17a**,**b** (see Scheme 6), both in vacuo (PM3 Hamiltonian)[24] and within a dielectric medium (using the COSMO solvation model).[25]

By analogy with previous theoretical studies,[5a,23] the reaction between the lithium azaenolate **16** and the 1-propenylphosphonates **17a**,**b** should involve an initial phosphoryl−lithium coordination to form the stable complexes **18a**,**b**. Subsequently, reorganization of these intermediates through competing eight-membered transition structures would initially afford the addition products as mixtures of the lithium phosphonate carbanions 2,5-*trans*-2,1′-*anti*-**19a** and 2,5-*trans*-2,1′-*syn*-**19b**, along with other minor isomers **20** with the 2,5-cis configuration. According to such a model, the diastereoselective formation of trans adducts must originate from a kinetic preference for the interaction through the *Re* face of the azaenolate (trans to the isopropyl group), while the syn/anti stereoselection relies on the energy difference between the possible transition structures resulting from the *like* or *unlike* approach of the azaenolate to the prochiral faces of the C*β* of the phosphonate.

We wished to employ a practical but reliable method applicable to the present problem but also to other molecular systems of future synthetic interest, considering larger alkenylphosphonates. Geometry optimization of such systems using *ab initio* or density functional theory methods may provide more accurate estimates, but are more demanding of computing capabilities. Hence, we have used semiempirical methods. Semiempirical calculations have progressed over the past few years to a surprising level of accuracy and reliability and nowadays are recognized as a rapid and useful tool in the elucidation of the reaction mechanisms of large molecular systems.[26] For this study, we have used the PM3 Hamiltonian,[24] which is generally superior to MNDO for the calculation of hypervalent molecules and appears to be particularly suited for mechanistic studies on large lithium amides and phosphonate carbanions.[27] Although the X-ray structure of a lithiated bis-lactim ether (derived from *cyclo*-[Ala-Ala]) has been determined as a trisolvated dimeric aggregate,[28] freezing-point depression measurements have shown an average degree of aggregation of 1.15 for the same compound at low-temperature diluted ethereal solutions.[29] Since lower reagent concentrations and higher solvent concentrations will promote reaction via the more highly solvated and less aggregated species, the azaenolate **16** was considered in this analysis to react as monomer, and complete dissociation of the possible oligomeric clusters in strong donor solvent was assumed. In this way, calculations in the gas phase have been performed with discrete solvation of lithium as working model. As water is an unrealistic ligand and is not generally suitable because of its tendency to hydrogen bond and dimethyl ether could originate crowded models for highly solvated species, we chose ethylene oxide as model for THF, which is conformationally more complex. Computations were also performed within a dielectric medium, mimicking the nonspecific solvation effect of THF.

We first examined the solvation equilibria for the monomeric azaenolate **16** in the gas phase (see Scheme 7). To estimate the solvent effect on the stability of **16**, complete geometry optimizations for unsolvated, monosolvated, disolvated, and trisolvated structures were carried out. In the unsolvated azaenolate **u16**, the lithium cation is stabilized by coordination with the vicinal methoxy group. This interaction is maintained in the mono and disolvated species **m16** and **d16**, respectively, but is lost in the trisolvated azaenolate **t16**. All

(22) Oare, D. A.; Henderson, M. A.; Sanner, M. A.; Heathkock, C. H. *J. Org. Chem.* **1990**, *55*, 133 and references therein.

(23) (a) Bernardi, A. *Gazz. Chim. Ital.* **1995**, *125*, 539. (b) Bernardi, A.; Capelli, A. M.; Cassinari, A.; Comotti, A.; Gennari, C.; Scolastico, C. *J. Org. Chem.* **1992**, *57*, 7029.

(24) Stewart, J. J. P. *J. Comput. Chem.* **1989**, *10*, 209, and 221. Lithium PM3 parameters: Anders, E.; Koch, R.; Freunscht, P. *J. Comput. Chem.* **1993**, *14*, 1301.

(25) Klamt, A.; Schüürmann, G. *J. Chem. Soc., Perkin Trans. 2* **1993**, 799.

(26) Stewart, J. J. P. Semiempirical Molecular Orbital Methods. In *Reviews in Computational Chemistry*; Lipkowitz, K. B., Boyd, D. B., Eds.; VCH: New York 1990; Vol. 1, p 45.

(27) (a) Hilmersson, G.; Arvidsson, P. I.; Davidsson, O.; Hakansson, M. *J. Am. Chem. Soc.* **1998**, *120*, 8143. (b) Koch, R.; Wiedel, B.; Anders, E. *J. Org. Chem.* **1996**, *61*, 2523. (c) Koch, R.; Anders, E. *J. Org. Chem.* **1995**, *60*, 5861.

(28) Seebach, D.; Bauer, W.; Hansen, J.; Laube, T.; Schweizer, W. B.; Dunitz, J. D. *J. Chem. Soc., Chem. Commun.* **1984**, 853.

(29) Bauer, W.; Seebach, D. *Helv. Chim. Acta* **1984**, *67*, 1972.

Scheme 7. Solvation Equilibria for Azaenolate 16[a]

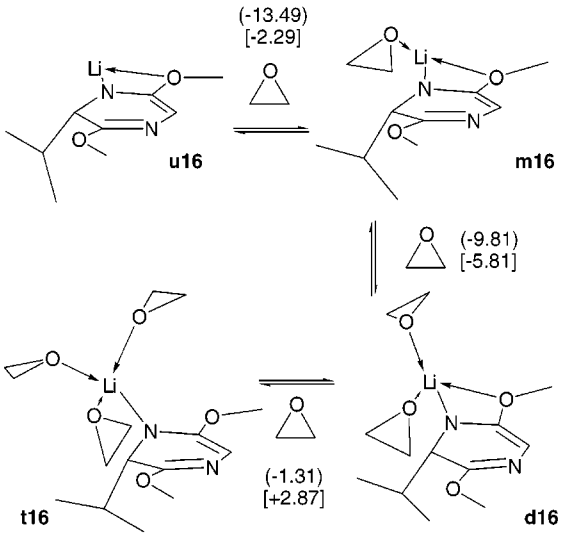

[a] Enthalpies in kcal/mol (gas-phase values in parentheses; condensed-phase values in brackets).

Scheme 8. Selected Solvation Equilibria for Coordination Complexes 18a,b[a]

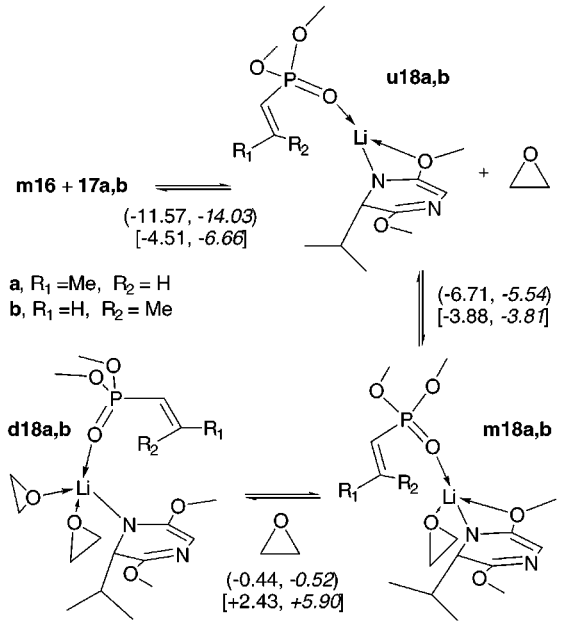

[a] Enthalpies in kcal/mol (gas-phase values are in parentheses; condensed-phase values are in brackets). Numbers for series a are on the left side, while numbers in italics are for series b).

the solvation enthalpies are negative. The first solvent molecule is the most effective: the heat of solvation is 13.49 kcal/mol, while the second and the third solvent molecules reduce the energy of the systems by only 9.81 and 1.31 kcal/mol, respectively. Higher solvated forms of the azaenolate were not examined, because of the small stabilization afforded by addition of the last solvent molecule.

In the gas phase, addition of azaenolate to propenylphosphonates **17a**,**b** proceeds first by the exothermic formation of the lithium-coordinated complexes **18a**,**b** shown in Scheme 8. These complexes are formed with no apparent reaction barriers. It is likely that in solution this coordination proceeds by replacement of a solvent molecule from the solvated azaenolate. The unsolvated (**u18a,b**) and monosolvated (**m18a,b**) complexes maintain the coordination between the lithium and vicinal methoxy groups, already shown by the parent azaenolates **m16** and **d16**. This interaction is not present in the disolvated complexes **d18a**,**b**. Lithium coordination requirements in the intermediate complexes are satisfied with only two solvent molecules, and the interaction with the vicinal methoxy group is no longer necessary. In this manner, the addition of the first solvent molecule is clearly exothermic, while the introduction of the second ligand reduces the enthalpy of the systems by less than 1 kcal/mol. Most stable conformations found for the complexes show the lithium atom above the plane of the pyrazine ring, providing a synclinal disposition between the lithium-coordinated phosphonate and the isopropyl group (trans coordination). Disolvated complexes also differ from the unsolvated and monosolvated ones by the geometry of the complexation. While disolvated structures show a positive NLiOP dihedral angle, approaching the propenyl moiety to one methoxy group (syn coordination), unsolvated and monosolvated complexes present a negative NLiOP dihedral angle, enabling an interaction between the propenyl and isopropyl groups (anti coordination).

Because of the reduced freedom of motion, each solvation process should also be unfavorable entropically. In this way, saturation of the lithium center on azaenolate−propenylphosphonate complexes by coordination to solvent is not necessarily a thermodynamically favored process. Thus, in addition to the disolvated complexes, with the lowest heats of formation, monosolvated species may also be important intermediates in the reaction pathway. In this way, we decided to analyze all possible rearrangements, considering both the mono- and the disolvated lithium-coordinated complexes. The reorganization of the intermediate complexes must enable the formation of a single bond connecting two chiral centers. Such rearrangements can proceed with four different configurations in the transition state. Thus, four different pathways, consequence of the interaction of both prochiral faces of the enolate and both prochiral faces of the acceptor, were initially considered for the rearrangement of mono- and disolvated complexes. As low energy conformations with either s-cis or s-trans configuration on the propenylphosphonate moiety were accessible for the all the lithium-coordinated complexes (**m18a**, **m18b**, **d18a**, and **d18b**), to compute all competitive transition structures eight different starting geometries were in fact studied for each complex. To define the potential energy profile for these rearrangements, the distance between the α-carbon of the enolate (C2) and the *β*-carbon of the propenylphosphonate (C1′) was used as the reaction coordinate. The reaction paths were calculated by systematically reducing the forming single bond length from 3.8 to 1.8 Å, while all the remaining geometrical parameters were optimized.

Full optimization of the geometries corresponding to the maximum potential energy along the selected paths in the rearrangement of **m18a**, the monosolvated complex derived from the (*E*)-1-propenylphosphonate, enabled the location of only four transition structures (**m21**−**24a**, see Figure 2), each one of them giving rise to a different stereoisomer of the addition product. These geometries, which maintain the coordination between lithium and

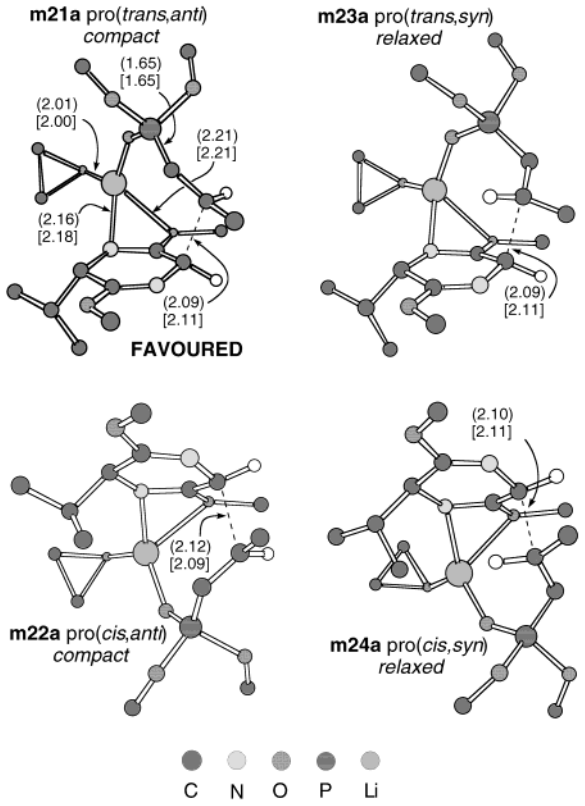

Figure 2. PM3-optimized geometries for the transition states located in the rearrangement of **m18a**. Distances in Å (gas-phase values are in parentheses and condensed-phase values are in brackets). Hydrogen atoms are omitted, except for the new stereocenters.

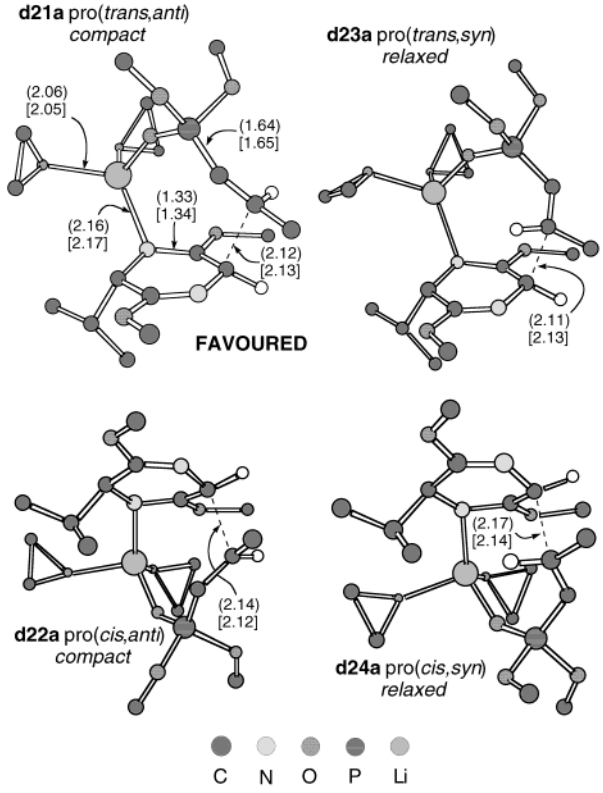

Figure 3. PM3-optimized geometries for the transition states located in the rearrangement of **d18a**. Distances in Å (gas-phase values are in parentheses and condensed-phase values are in brackets). Hydrogen atoms are omitted, except for the new stereocenters.

vicinal methoxy group, show almost the same C(2)C(1′) bond distance (between 2.09 and 2.12 Å), an anticlinal C(2)C(3)NLi angle (ca. 137°), and a synperiplanar LiOPC angle (lower than 5°). A synclinal conformation at the CCPO moiety is also found in all the transition structures, suggesting that the addition actually takes place by azaenolate attack on the acceptor moiety with an s-cis oriented phosphoryl group.

Similar study of the rearrangement of **d18a**, the disolvated complex derived from the (*E*)-1-propenylphosphonate, also led to the location of four diastereomeric transition structures **d21**−**24a** (see Figure 3). The disolvated transition states showed almost the same values for the forming CC bond length and the CCNLi, LiOPC, and CCPO dihedral angles as the monosolvated ones. The *procis* disolvated transition structures, **d22a** and **d24a**, presented a weak interaction between the lithium cation and the vicinal methoxy group (binding distances longer than 2.38 Å), while the *protrans* ones, **d21a** and **d23a**, are characterized by the absence of such coordination. Both in the mono- and disolvated series, the geometries resulting from the *like* and *unlike* approaches of the azaenolate moiety to the Cβ of the propenyl group clearly differ in sense of the synclinal arrangement around the forming CC bond. The *like* approximations resulted in *compact* dispositions[30] of the donor/acceptor moieties (models **m21a** and **m22a** in Figure 2 and **d21a** and **d22a** in Figure 3), while the optimization of the *unlike* ones yielded geometries with a *relaxed* propenyl/pyrazine interaction (models **m23a** and **m24a** in Figure 2, and **d23a** and **d24a** in Figure 3). As for the (*E*)-propenyl-derived transition states, the *compact* approaches result in anti configuration (while the *relaxed* ones afford the syn relationship), the orientation of the propenyl group with respect to the azaenolate moiety is the responsible for the energetic differentiation of the *prosyn*/*proanti* diastereomeric transition structures. In addition, in both the mono- and disolvated series, the two *protrans* transition states were determined to be lower in energy than the corresponding *procis*, conveniently correlating the high face-selectivity showed by lithiated bis-lactim ethers in Michael additions (see Table 2). Thus, PM3 calculations determine the *compact pro(trans,anti)* geometries **m21a** and **d21a** as the most favored, in accordance with the experimental trend. Moreover, the differences of activation enthalpies between the *compact pro(trans,anti)* geometries and any of the most favored *procis* or *prosyn* transition structures are in agreement with the observed diastereomeric ratios.

Following the same strategy for the analysis of the rearrangement of the (*Z*)-propenyl derived intermediate complexes **m18b** and **d18b**, similar results were obtained. Full optimization of the selected starting geometries also led to the location of four diastereomeric transition structures in each of the solvation series: **m21**−**24b** and **d21**−**24b** (only the disolvated geometries are shown in Figure 4). All transition structures are characterized by a similar length in the forming single CC bond (2.07−2.14 Å) and an antiperiplanar, syn-

(30) A *compact* approach was also proposed in other conjugate additions: (a) Cavé, C.; Desmaële, D.; d'Angelo, J.; Riche, C.; Chiaroni, A. *J. Org. Chem.* **1996**, *61*, 4361. (b) Sevin, A.; Tortajada, J.; Pfau, M. *J. Org. Chem.* **1986**, *51*, 2671.

Table 2. Heats of Formation, Energy Barriers (kcal/mol), and Imaginary Frequencies (cm^{-1}) for the Transition Structures Located in the Addition of 16 to (*E*)-Propenylphosphonate 17a, in Vacuo ($\epsilon = 1$, PM3), or a Polarizable Dielectric Continuum ($\epsilon = 12.13$, PM3/COSMO)

		$\epsilon = 1$				$\epsilon = 12.13$			
compd	confign	$\Delta H°$	ni(vi)	$\Delta^{\ddagger}H°$	$\Delta\Delta^{\ddagger}H°$	$\Delta H°$	ni(vi)	$\Delta^{\ddagger}H°$	$\Delta\Delta^{\ddagger}H°$
m21a	trans,anti	−240.46	1 (−405.1)	22.21	0.00	−250.17	1 (−466.2)	28.31	0.00
m22a	cis,anti	−237.12	1 (−394.6)		3.34	−247.66	1 (−477.3)		2.51
m23a	trans,syn	−239.07	1 (−395.1)		1.39	−248.48	1 (−459.9)		1.69
m24a	cis,syn	−238.44	1 (−238.4)		2.02	−248.36	1 (−483.1)		1.81
d21a	trans,anti	−252.16	1 (−403.6)	18.68	0.00	−263.13	1 (−462.1)	25.44	0.00
d22a	cis,anti	−247.73	1 (−386.6)		4.42	−259.47	1 (−481.2)		3.66
d23a	trans,syn	−250.30	1 (−397.4)		1.85	−260.50	1 (−459.2)		2.63
d24a	cis,syn	−247.88	1 (−382.9)		4.28	−260.01	1 (−470.3)		3.12

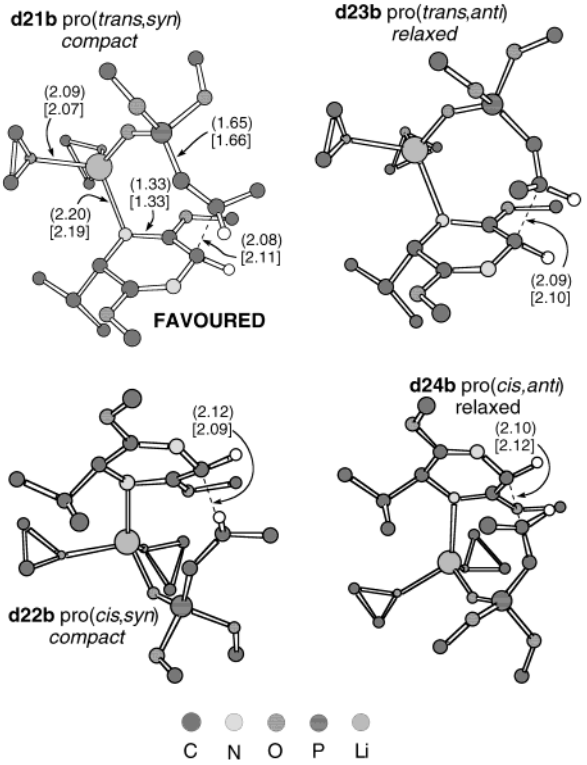

Figure 4. PM3-optimized geometries for the transition states located in the rearrangement of **d18b**. Distances in Å (gas-phase values are in parentheses and condensed-phase values are in brackets). Hydrogen atoms are omitted, except for the new stereocenters.

periplanar, and synclinal conformation for the CCNLi, LiOPC, and CCPO moieties, respectively. The *protrans* disolvated transition structures of this series also showed no coordination between the lithium cation and the vicinal methoxy group. As previously calculated for the rearrangement of the complexes derived from (*E*)-1-propenylphosphonates, the *protrans* transition states were determined to be more stable than their *procis* counterparts, and the *like* and *unlike* approximations were also optimized to energetically differentiated *compact* and *relaxed* geometries. Again, PM3 calculations showed a kinetic preference for a *compact* disposition of the reaction couple in the transition structures. Nevertheless, in this case, the *compact* geometries presented an *ul* topicity, enabling the reversal of the π-face selectivity of the rearrangement. Thus, the energy gap between the *pro(trans,syn)* and the competing diastereomeric transition states conveniently reproduces the sense and degree of the stereoselection in the additions to (*Z*)-propenylphosphonates (see Table 3).

Although some uncertainty remains resulting from the PM3 tendency to overestimate the stability of the initially formed complexes,[31] the activation barriers to the rearrangement in both (*E*)- and (*Z*)-series appear to decrease under the influence of solvent molecules. Thus, in the gas phase, the reaction paths involving disolvated intermediate complexes and disolvated transition structures seems to be favored over those with participation of monosolvated species ($\Delta\Delta^{\ddagger}H$(mono-di) = 3.53 and 1.08 kcal/mol in the (*E*)- and (*Z*)-propenyl series, respectively).

To further study the influence of the solvent in the reaction path, the geometries of all intermediates and transition states as calculated in vacuo were reoptimized in a dielectric medium simulating THF using the COSMO technique.[25] The effect of the dielectric medium on the structures of azaenolates, chelate complexes, and transition structures was rather small, with solvent-induced bond length changes up to 0.03 Å. Nevertheless, the solvation equilibria and the energetic profile for the rearrangement in the dielectric medium clearly differ from those encountered in the gas phase. Nonspecific solvation has a significant stabilizing effect on the energies of all the structures. In addition, enthalpies of solvation were calculated lower in the dielectric continuum than in the gas phase. Thus, in THF, the solvation equilibria for the azaenolates and coordination complexes seem to be dominated by the disolvated and monosolvated species, **d16** and **m18a**,**b**, respectively (see Schemes 7 and 8). Nonspecific solvation of the transition states (with less charge-localized geometries) was to be less exothermic than that for the coordination complexes, thus increasing the enthalpies of activation for the rearrangement by ca. 6 kcal/mol (see Tables 2 and 3). Differential nonspecific solvation effects on the competitive transition states are also rather small, and thus the differences in energy between the reoptimized transition structures also correlates with the experimental stereoselection in the conjugate addition to either (*Z*)- and (*E*)-1-propenylphosphonates.

Conclusion

In conclusion, the conjugate additions of metalated Schöllkopf's bis-lactim ethers to 1-propenylphosphonates take place regio- and stereoselectively. The reaction results in an almost complete translation of the *Z*/*E* geometry into a syn/anti configuration at the 1,4-addition products. In this way, the stereochemical outcome of the conjugate addition is shown to be both reagent- and substrate-controlled. While the influence of the chiral

(31) Opitz, A.; Koch, R.; Katritzky, A. R.; Fan, W.-Q.; Anders, E. *J. Org. Chem.* **1995**, *60*, 3743.

Table 3. Heats of Formation, Energy Barriers (kcal/mol), and Imaginary Frequencies (cm^{-1}) for the Transition Structures Located in the Addition of 16 to (*Z*)-Propenylphosphonate 17b, in Vacuo ($\epsilon = 1$, PM3), or a Polarizable Dielectric Continuum ($\epsilon = 12.13$, PM3/COSMO)

		$\epsilon = 1$				$\epsilon = 12.13$			
compd	confign	$\Delta H°$	ni(vi)	$\Delta^{\ddagger}H°$	$\Delta\Delta^{\ddagger}H°$	$\Delta H°$	ni(vi)	$\Delta^{\ddagger}H°$	$\Delta\Delta^{\ddagger}H°$
m21b	trans,syn	−236.32	1 (−409.5)	21.07	0.00	−247.80	1 (−476.6)	27.87	0.00
m22b	cis,syn	−234.31	1 (−403.5)		2.01	−245.53	1 (−481.3)		2.26
m23b	trans,anti	−232.73	1 (−402.2)		3.59	−242.73	1 (−477.4)		5.07
m24b	cis,anti	−232.36	1 (−401.6)		3.96	−243.88	1 (−489.2)		3.92
d21b	trans,syn	−246.09	1 (−413.9)	19.99	0.00	−256.66	1 (−484.5)	33.13	0.00
d22b	cis,syn	−244.30	1 (−396.9)		1.78	−255.98	1 (−465.7)		0.68
d23b	trans,anti	−244.75	1 (−406.1)		1.34	−255.38	1 (−457.4)		1.28
d24b	cis,anti	−240.01	1 (−408.2)		5.97	−251.80	1 (−472.6)		4.76

glycine equivalent determines the absolute stereochemistry, the relative configuration at the addition products exclusively depends on the geometry of the acceptor. In addition, a semiempirically optimized model that rationalizes the stereochemical course of the conjugate addition has been devised. Both PM3 and PM3/COSMO calculations support the rate-determining reorganization of intermediate chelate complexes through competitive eight-membered transition states. According to this model, the stereochemical response of the conjugate addition to the acceptor geometry originates from an orientational preference in the cyclic transition states for a *compact* disposition of the reaction partners. The level of π-facial discrimination delivered by the metalated azaenolate/1-propenylphosphonate couple enables a stereocontrolled access to 2-amino-3-methyl-4-phosphonobutanoic acids, which may result in useful tools for determining the requirements for receptor binding and physiological responses at mGluRs of group III.

Experimental Section

Computational Methods. All calculations have been performed using the MOPAC 97[32] module of Chem3D Pro program.[33] All structures were fully optimized at the restricted Hartree−Fock level of theory with the PM3 method,[24] using the eigenvector following routine (TS keyword for transition-state refinement) under the more rigorous criteria of the keyword PRECISE (gradient norm < 0.03). Solvent dielectric effects of THF were simulated with the COSMO technique,[25] using a relative permittivity of 12.13 for THF at −78 °C[34] (keyword EPS = 12.13, with RSOLV = 2 to account for the larger size of THF with respect to water), and using 60 surface segments per atom to construct a solvent-accessible surface area based on van der Waals radii (keyword NSPA = 60). Maxima were characterized as first-order transition structures by normal-mode analyses, yielding a single imaginary frequency, and their nature was verified by internal reaction coordinate calculations to reactants and products. Conformational space accessible for each of the reported transition structures was studied in the following way: two different rotamers for the isopropyl group (those with the tertiary carbon pointing to the lithium atom, or pointing to the imidate moiety), three rotamers for each solvent molecule (located by performing grid (3 × 3) calculations on disolvated species), and all the gauche-gauche conformations for the COPOC moiety were analyzed. In the study of the conformational space accessible to the coordination complexes, a systematic search on CCNLi, CNLiO, and NLiOP dihedral angles with a step size of 120° was performed first, starting from geometries with syn or anti coordination (with respect to the isopropyl group) and s-cis or s-trans configuration at the CCPO moiety. Only for the most important conformers located in this search the isopropyl and COPOC rotamers were also studied.

General Methods. All moisture-sensitive reactions were performed under an argon atmosphere using oven-dried glassware. Reagents and solvents were purchased and used without further purification unless otherwise stated. HMPA was dried over 4 Å molecular sieves, THF was distilled from sodium/benzophenone, and CH_2Cl_2 was distilled from calcium hydride. Reactions were monitored by thin-layer chromatography carried out on 0.25 mm E. Merck silica gel plates (60F-254) using iodine or ninhydrin as developing agents. E. Merck silica gel 60 and RP-18 (both 230−400 mesh) were used for liquid chromatography separations. Melting points are uncorrected. IR spectra were obtained as liquid film or as KBr pellets. Unless otherwise indicated, ^{1}H NMR spectra were recorded at 360 MHz. ^{13}C NMR and ^{31}P NMR spectra were recorded at 90.6 and 145.8 MHz, respectively, with broad-band ^{1}H decoupling. Recognition of methyl, methylene, methine, and quaternary carbon nuclei in ^{13}C spectra rests on the *J*-modulated spin-echo sequence. ^{1}H and ^{13}C assignments were confirmed with the aid of ^{13}C,^{1}H 2D-correlation experiments, as previously described.[35] In the carbon spectra, all peaks for which a coupling constant is reported are doublets due to phosphorus coupling. Mass spectra (EI) were obtained with an ionization voltage of 70 eV, and FABMS spectra were recorded using thioglycerol as a matrix. Elemental analyses were performed at Servicios Xerais de Apoio á Investigación of Universidade da Coruña.

Multigram quantities of both enantiomers of 2,5-diethoxy-3-isopropyl-3,6-dihydropyrazine were obtained from Novartis kilo laboratory. Diethyl (*Z*)-1-propenylphosphonate (**4b**) was prepared as reported. [11]

Diethyl 2-Bromopropylphosphonate (8). A mixture of triethyl phosphite (15 g, 90 mmol) and 1,2-dibromopropane (57 mL, 547 mmol) was heated to reflux for 14 h under an argon atmosphere. After removal of the excess of dibromopropane in vacuo, Kugelrohr distillation of the residue gave 16.3 g (70%) of bromophosphonate **8** as a colorless oil: bp 90 °C (0.13 mbar); R_f 0.52 (silica gel, AcOEt/hexane 2:1); IR (film) ν 1250 (P═O), 1055, 1027, 963 (POC), 509 (CBr) cm^{-1}; ^{1}H NMR ($CDCl_3$) δ 1.34 (t, J = 7.1 Hz, 6H), 1.85 (d, J = 6.6 Hz, 3H), 2.38 (ddd, J = 17.8, 15.3, 9.3 Hz, 1H), 2.56 (ddd, J = 19.7, 15.3, 5.0 Hz, 1H), 4.07−4.17 (m, 4H), 4.35−4.47 (m, 1H); ^{13}C NMR ($CDCl_3$) δ 16.4 (J = 6.2 Hz, CH_3), 27.4 (J = 5.1 Hz, CH_3), 38.2 (J = 134.7 Hz, CH_2), 41.7 (CH), 61.8 (J = 6.5 Hz, CH_2), 62.0 (J = 6.5 Hz, CH_2); ^{31}P NMR ($CDCl_3$) δ 25.55; EIMS *m*/*z* 261/259 (M^+, 100/100), 179 (M^+ − Br, 98), (M^+ − C_4H_9Br, 95).

Diethyl (*E*)-1-Propenylphosphonate (4a). DBU (12.9 mL, 86.2 mmol) was added dropwise over a cooled (0 °C) solution of bromophosphonate **8** (15 g, 57.7 mmol) in CH_2Cl_2 (180 mL). The mixture was stirred for 1 h, the solvent was evaporated, and the crude product was purified by flash chromatography (silica gel, AcOEt/hexane 2:1−3:1) to give **4a** (8.7 g, 85%) as a colorless oil: R_f 0.33 (silica gel, AcOEt/hexane 2:1); ^{1}H NMR (200 MHz, $CDCl_3$) δ 1.27 (t, J = 7.2 Hz, 6H),

(32) Revised version of MOPAC93, Fujitsu Ltd, Tokyo, Japan 1993.
(33) CS Chem3D Pro, version 4.0; Molecular Modeling and Analysis Program; CambridgeSoft Corporation: Cambridge, MA 02139, 1997.
(34) Carvajal, C.; Tölle, K. J.; Smid, J.; Szwarc, M. *J. Am. Chem. Soc.* **1965**, *87*, 5548.
(35) Pombo-Villar, E.; Boelsterli, J.; Cid, M. M.; France, J.; Fuchs, B.; Walkinshaw, M.; Weber, H.-P. *Helv. Chim. Acta* **1993**, *76*, 1203 and pertinent references therein.

1.87 (ddd, J = 6.8, 2.3 Hz, 3H), 4.02−4.17 (m−dq, 4H), 5.62 (ddq, J = 21.0, 16.6, 2.3 Hz, 1H), 6.74 (ddq, J = 21.5, 16.6, 6.8 Hz, 1H).

General Procedure for Michael Additions of Metalated Schöllkop's Bis-lactim Ethers to 1-Propenylphosphonates. Method A. A solution of *n*-BuLi (1.0−3.0 equiv, 2.5 M in hexane) was added to a stirred solution of the bis-lactim ether in THF (1.0−3.0 equiv, 10 mL/mmol) at −78 °C, and the mixture was stirred for 1 h. Then, a solution of the propenyl phosphonate **4a**,**b** or a mixture of bromophosphonate **8** and propenylphosphonate **4a** (1.0 equiv, see Table 1, entries 1, 2, 9, 10, and 12−17) in THF (2 mL/mmol) was added dropwise. After being stirred at −78 °C for 5 min, the reaction was quenched with AcOH. The crude reaction mixture was warmed to room temperature, and the solvent was removed in vacuo. The resulting material was diluted with water and extracted with AcOEt. The combined organic layers were dried (Na_2SO_4) and evaporated, and the residue was purified by gradient flash chromatography (silica gel, AcOEt/hexane 2:1−4:1) to yield pure adducts as colorless oils. **Method B.** A solution of *n*-BuLi (1.0 or 2.0 equiv, 2.5 M in hexane) was added to a stirred solution of the bis-lactim ether (1.0 or 2.0 equiv) in THF (10 mL/mmol) at −78 °C, and the mixture was stirred for 1 h. Then, a solution of the additive (12-crown-4, HMPA, $SnCl_2$, $CuBr_2{\cdot}SMe_2$, $TiCl(O^iPr)_3$ or $MgBr_2{\cdot}OEt_2$, see Table 1, entries 3−8 and 11) in THF was added. The mixture was stirred for 1 h, and a solution of propenylphosphonate **4a** (1.0 equiv) in THF (2 mL/mmol) was added dropwise. After being stirred at −78 °C for 5 min (or warming up to 0 °C for 10 h, see Table 1, entries 5 and 6) the reaction was quenched with AcOH and worked up as described in method A.

(2*S*,5*R*,1′*R*)-3,6-Diethoxy-2-[2-(diethoxyphosphoryl)-1-(methyl)ethyl]-2,5-dihydro-5-isopropylpyrazine ((+)-10a). Propenylphosphonate **4a** (10.35 g, 58.1 mmol) and (3*R*)-2,5-diethoxy-3-isopropyl-3,6-dihydropyrazine (22.4 g, 105.5 mmol) were allowed to react according to the general procedure (method A), yielding after column chromatography 13.4 g of (+)-**10a** (59%) as a colorless oil: R_f 0.46 (silica gel, AcOEt); $[\alpha]^{20}_D$ = +24.3 (*c* 1.0, CH_2Cl_2); IR (film) ν 1690 (C=N), 1237 (P=O), 1059, 1030 (POC) cm^{-1}; ^1H NMR ($CDCl_3$) δ 0.69 (d, J = 6.8 Hz, 3H, $CH(CH_3)_2$), 1.02 (d, J = 6.8 Hz, 3H, $CH(CH_3)_2$), 1.21 (d, J = 6.8 Hz, 3H, $CHCH_3$), 1.25−1.36 (m, 12H, OCH_2CH_3), 1.45−1.52 (m, 2H, H-2′), 2.25 (dsp, J = 6.8, 3.0 Hz, 1H, $CH(CH_3)_2$), 2.51−2.65 (m, 1H, $CH(CH_3)$), 3.86−3.91 (m, 2H, H-2, H-5), 4.00−4.22 (m, 8H, OCH_2); ^{13}C NMR ($CDCl_3$) δ 14.3 (OCH_2CH_3), 16.4 (J = 6.2 Hz, $POCH_2CH_3$), 16.6 ($CH(CH_3)_2$), 17.1 ($CHCH_3$), 19.0 ($CH(CH_3)_2$), 27.8 (J = 141.0 Hz, C-2′), 32.0 ($CH(CH_3)_2$, C-1′), 60.6 (J = 11.9 Hz, C-2), 60.6 (OCH_2CH_3), 60.7 (C-5), 60.9 (OCH_2CH_3), 61.2 (J = 6.4 Hz, $POCH_2CH_3$), 61.4 (J = 6.4 Hz, $POCH_2CH_3$), 161.9 (CN), 163.5 (CN); ^{31}P NMR ($CDCl_3$) δ 32.91; FABMS *m*/*z* 391 (MH^+, 100). Anal. Calcd for $C_{18}H_{35}N_2O_5P$: C, 55.37; H, 9.04; N. 7.17. Found: C, 55.65; H, 8.89; N, 7.41.

(2*R*,5*S*,1′*S*)-3,6-Diethoxy-2-[2-(diethoxyphosphoryl)-1-(methyl)ethyl]-2,5-dihydro-5-isopropylpyrazine ((−)-10a) was prepared following the same procedure, from **4a** (7.1 g, 40.0 mmol) and (3*S*)-2,5-diethoxy-3-isopropyl-3,6-dihydropyrazine (25.5 g, 120.1 mmol), to yield 12.8 g (82%) of a colorless oil: $[\alpha]^{20}_D$ = −24.3 (*c* 1.0, CH_2Cl_2).

(2*S*,5*R*,1′*S*)-3,6-Diethoxy-2-[2-(diethoxyphosphoryl)-1-(methyl)ethyl]-2,5-dihydro-5-isopropylpyrazine ((−)-10b). Propenylphosphonate **4b** (2.4 g, 13.47 mmol) and (3*R*)-2,5-diethoxy-3-isopropyl-3,6-dihydropyrazine (8.58 g, 40.41 mmol) were allowed to react according to the general procedure (method A), yielding after column chromatography 4.34 g of (−)-**10b** (83%) as a colorless oil: R_f 0.46 (silica gel, AcOEt); $[\alpha]^{20}_D$ = −14.6 (*c* 1.1, CH_2Cl_2); IR (film) ν 1692 (C=N), 1236 (P=O), 1058, 1033 (POC) cm^{-1}; ^1H NMR ($CDCl_3$) δ 0.70 (d, J = 6.8 Hz, 3H, $CH(CH_3)_2$), 0.77 (d, J = 6.8 Hz, 3H, $CHCH_3$), 1.02 (d, J = 6.8 Hz, 3H, $CH(CH_3)_2$), 1.26 (t, J = 7.1 Hz, 3H, OCH_2CH_3), 1.27 (t, J = 7.1 Hz, 3H, OCH_2CH_3), 1.32 (t, J = 7.1 Hz, 3H, OCH_2CH_3), 1.33 (t, J = 7.1 Hz, 3H, OCH_2CH_3), 1.80 (ddd, J = 17.8, 15.5, 7.6 Hz, 1H, H-2′), 2.16 (ddd, J = 18.2, 15.5, 6.2 Hz, 1H, H-2′), 2.24 (dsp, J = 6.8, 3.5 Hz, 1H, $CH(CH_3)_2$), 2.63−2.71 (m, 1H, H-1′), 3.89 (t, J = 3.5 Hz, 1H, H-5), 4.04 (t, J = 3.5 Hz, 1H, H-2), 4.08−4.20 (m, 8H, OCH_2); ^{13}C NMR ($CDCl_3$) δ 14.3 (OCH_2CH_3), 14.4 (OCH_2CH_3), 15.3 (J = 9.7 Hz, $CHCH_3$), 16.4 (J = 6.2 Hz, $POCH_2CH_3$), 16.7 ($CH(CH_3)_2$), 19.0 ($CH(CH_3)_2$), 29.2 (J = 139.3 Hz, C-2′), 31.1 (J = 2.5 Hz, C-1′), 32.1 ($CH(CH_3)_2$), 59.0 (J = 11.3 Hz, C-2), 60.4 (OCH_2CH_3), 60.5 (OCH_2CH_3), 60.8 (C-5), 61.4 (J = 6.4 Hz, $POCH_2CH_3$), 162.1 (CN), 163.4 (CN); ^{31}P NMR ($CDCl_3$) δ 33.00; FABMS *m*/*z* 391 (MH^+, 100). Anal. Calcd for $C_{18}H_{35}N_2O_5P$: C, 55.37; H, 9.04; N. 7.17. Found: C, 55.59; H, 9.23; N, 6.99.

(2*R*,5*S*,1′*R*)-3,6-Diethoxy-2-[2-(diethoxyphosphoryl)-1-(methyl)ethyl]-2,5-dihydro-5-isopropylpyrazine ((+)-10b) was prepared following the same procedure, from **4b** (3.0 g, 16.8 mmol) and (3*S*)-2,5-diethoxy-3-isopropyl-3,6-dihydropyrazine (10.7 g, 50.4 mmol), to yield 5.37 g (82%) of a colorless oil: $[\alpha]^{20}_D$ = +14.5 (*c* 1.0, CH_2Cl_2).

Ethyl (2*S*,3*R*)-2-Amino-4-diethoxyphosphoryl-3-methylbutanoate ((+)-12a). A solution of adduct (+)-**10a** (9.37 g, 24.0 mmol) in 200 mL of THF and 240 mL of 0.25 N HCl was stirred at room temperature for 24 h. Then, the solvent was evaporated to half its initial volume (below 40 °C), and the aqueous solution was made basic (pH ∼10) by the addition of $NaHCO_3$ followed by concentrated ammonia. The aqueous layer was extracted with CH_2Cl_2, and the combined organic layers were dried (Na_2SO_4) and evaporated. The crude mixture of methyl valinate and amino ester (+)-**12a** was purified by flash chromatography (silica gel, AcOEt to AcOEt/MeOH 8:1) to yield 6.4 g (95%) of (+)-**12a** as a colorless oil: R_f 0.36 (silica gel, AcOEt/MeOH 10:1); $[\alpha]^{20}_D$ = +10.6 (c 1.0, CH_2Cl_2); IR (film) ν 3375, 3280 (NH_2), 1732 (C=O), 1243 (CO, P=O), 1057, 1028 (POC) cm^{-1}; ^1H NMR ($CDCl_3$) δ 1.11 (d, J = 6.8 Hz, 3H), 1.26 (t, J = 7.1 Hz, 3H), 1.30 (t, J = 7.1 Hz, 6H), 1.58 (brs, 2H), 1.61 (ddd, J = 17.9, 15.3, 10.1 Hz, 1H), 2.01 (ddd, J = 18.5, 15.3, 3.2 Hz, 1H), 2.16−2.32 (m, 1H), 3.32 (dd, J = 5.2, 1.0 Hz, 1H), 4.04−4.10 (m, 4H), 4.17 (dq, J = 7.1, 1.7 Hz, 2H); ^{13}C NMR ($CDCl_3$) δ 14.3 (CH_3), 16.4 (J = 6.1 Hz, CH_3), 17.4 (J = 3.3 Hz, CH_3), 28.1 (J = 141.0 Hz, CH_2), 32.9 (J = 3.0 Hz, CH), 59.6 (J = 16.1 Hz, CH), 60.9 (CH_2), 61.4 (J = 6.4 Hz, CH_2), 61.5 (J = 6.4 Hz, CH_2), 174.7 (CO); ^{31}P NMR ($CDCl_3$) δ 31.96; FABMS *m*/*z* 282 (MH^+, 100).

Ethyl (2*R*,3*S*)-2-amino-4-diethoxyphosphoryl-3-methylbutanoate ((−)-12a) was prepared following the same procedure, starting from 5.5 g of adduct (−)-**10a** to yield 3.56 g (90%) of a colorless oil: $[\alpha]^{20}_D$ = −10.7 (*c* 1.0, CH_2Cl_2). Anal. Calcd for $C_{11}H_{24}NO_5P$: C, 46.97; H, 8.60; N. 4.98. Found: C, 46.69; H, 8.45; N, 5.08.

Ethyl (2*S*,3*S*)-2-Amino-4-diethoxyphosphoryl-3-methylbutanoate ((+)-12b). Amino ester (+)-**12b** was prepared as described above for the 2,3-anti isomers, starting from 2.6 g of adduct (−)-**10b** to yield 1.74 g (93%) of a colorless oil: R_f 0.38 (silica gel, AcOEt/MeOH 10:1); $[\alpha]^{20}_D$ = +20.5 (*c* 1.0, CH_2Cl_2); IR (film) ν 3375, 3280 (NH_2), 1733 (C=O), 1240 (CO, P=O), 1056, 1028 (POC) cm^{-1}; ^1H NMR ($CDCl_3$) δ 0.94 (dd, J = 6.9, 1.0 Hz, 3H), 1.27 (t, J = 7.1 Hz, 3H), 1.34 (t, J = 7.1 Hz, 3H), 1.35 (t, J = 7.1 Hz, 3H), 1.55 (brs, 2H), 1.70 (ddd, J = 22.5, 15.4, 7.1 Hz, 1H), 2.02 (ddd, J = 22.3, 15.4, 6.9 Hz, 1H), 2.39−2.53 (m, 1H), 3.64 (d, J = 3.5 Hz, 1H), 4.03−4.15 (m, 4H), 4.18 (dq, J = 7.1, 2.7 Hz, 2H); ^{13}C NMR ($CDCl_3$) δ 14.2 (CH_3), 15.3 (J = 11.1 Hz, CH_3), 16.4 (J = 6.1 Hz, CH_3), 29.6 (J = 139.8 Hz, CH_2), 31.7 (CH), 57.7 (J = 10.4 Hz, CH), 60.9 (CH_2), 61.4 (J = 6.4 Hz, CH_2), 174.9 (CO); ^{31}P NMR ($CDCl_3$) δ 31.44; FABMS (thioglycerol) *m*/*z* 282 (MH^+, 100). Anal. Calcd for $C_{11}H_{24}NO_5P$: C, 46.97; H, 8.60; N. 4.98. Found: C, 47.17; H, 8.88; N, 5.12.

Ethyl (2*R*,3*R*)-2-amino-4-diethoxyphosphoryl-3-methylbutanoate ((−)-12b) was prepared following the same procedure, starting from 3.7 g of adduct (+)-**10b** to yield 2.45 g (92%) of a colorless oil: $[\alpha]^{20}_D$ = −20.4 (*c* 1.0, CH_2Cl_2).

(2*S*,3*R*)-2-Amino-3-methyl-4-phosphonobutanoic Acid ((+)-6a). A solution of amino ester (+)-**12a** (360 mg, 1.28 mmol) was heated to reflux for 5 h in 7 mL of HCl 12 N. The solvent was evaporated under reduced pressure, and the amino acid hydrochloride was dried in vacuo overnight (10^{-3} mbar, 50 °C). The residue was dissolved in 4 mL of absolute EtOH, and propylene oxide (4 mL) was added dropwise. The white

precipitate immediately formed was filtered, dried, and purified by reversed-phase flash chromatography, eluting with water to give (+)-**6a** (236 mg, 94%) as a colorless solid: mp (EtOH) > 80 °C (dec); R_f 1.0 (RP-18, H_2O); $[\alpha]^{20}_D = +33.8$ (*c* 1.0, H_2O); IR (KBr) ν 3430 (OH), 2976 (NH_2), 1727 (C═O), 1257 (CO), 1122 (P═O), 1040, 931 (POH) cm^{-1}; ^1H NMR (D_2O) δ 1.16 (d, $J = 6.8$ Hz, 3H, CH_3), 1.77 (ddd, $J = 18.1$, 15.3, 9.1 Hz, 1H, H-4), 1.82 (ddd, $J = 19.2$, 15.3, 6.1 Hz, 1H, H-4), 2.45−2.58 (m, 1H, H-3), 4.08 (d, 3.6 Hz, 1H, H-2); ^{13}C NMR (D_2O) δ 18.7 ($J = 6.4$ Hz, CH_3), 33.1 (C-3), 33.8 ($J = 128.8$ Hz, C-4), 61.0 ($J = 12.8$ Hz, C-2), 174.3 (CO); ^{31}P NMR (D_2O) δ 23.80; FABMS *m*/*z* 198 (MH^+, 100), 152 ($[M - CO_2]H^+$, 18).

(2*R*,3*S*)-2-Amino-3-methyl-4-phosphonobutanoic acid ((−)-6a) was prepared following the same procedure, starting from 620 mg of amino ester (−)-**12a** to yield 378 mg (89%) of a colorless solid: $[\alpha]^{22}_D = -34.2$ (*c* 1.0, H_2O).

(2*S*,3*S*)-2-Amino-3-methyl-4-phosphonobutanoic Acid ((+)-6b). Amino acid (+)-**6b** was prepared following the same procedure as described above for the 2,3-*anti*-amino acids **6a**, starting from 500 mg of amino ester (+)-**12b** to yield 321 mg (91%) of a colorless solid: mp (EtOH) > 80 °C (dec); R_f 1.0 (RP-18, H_2O); $[\alpha]^{20}_D = +14.2$ (*c* 1.0, H_2O); IR (KBr) ν 3441 (OH), 3275 (NH_2), 1733 (C═O), 1257 (C−O), 1030, 920 (POH) cm^{-1}; ^1H NMR (D_2O) δ 1.15 (d, $J = 7.1$ Hz, 3H, CH_3), 1.74 (ddd, $J = 18.5$, 15.3, 7.8 Hz, 1H, H-4), 1.87 (ddd, $J = 18.7$, 15.3, 6.1 Hz, 1H, H-4), 2.55−2.70 (m, 1H, H-3), 4.08 (d, $J = 3.4$ Hz, 1H, H-2); ^{13}C NMR (D_2O) δ 18.6 ($J = 6.4$ Hz, CH_3), 32.9 (C-3), 33.7 ($J = 132.5$ Hz, C-4), 61.2 ($J = 6.0$ Hz, C-2), 174.7 (CO); ^{31}P NMR (D_2O) δ 23.80; FABMS *m*/*z* 198 (MH^+, 100), 152 ($[M - CO_2]H^+$, 25).

(2*R*,3*R*)-2-Amino-3-methyl-4-phosphonobutanoic acid ((−)-6b) was prepared following the same procedure, starting from 600 mg of amino ester (−)-**12b** to yield 389 mg (92%) of a colorless solid: $[\alpha]^{20}_D = -13.9$ (*c* 1.0, H_2O).

Ethyl (2*R*,3*S*)-2-[*N*-(*tert*-Butoxycarbonyl)amino]-4-diethoxyphosphoryl-3-methylbutanoate (14a). A solution of the amino ester (−)-**12a** (2.0 g, 7.1 mmol), Na_2CO_3 (566 mg, 5.34 mmol), and $NaHCO_3$ (532 mg, 6.34 mmol) in 50 mL of dioxane and 50 mL of H_2O at 0 °C was treated with Boc_2O (1.8 g, 8.31 mmol). The mixture was stirred at room temperature for 1 h, after which time it was concentrated to half its initial volume and extracted with CH_2Cl_2. The combined organic layers were dried (Na_2SO_4) and concentrated in vacuo. The crude material was purified by flash chromatography (silica gel, AcOEt/hexane 3:1 to AcOEt) to give 2.57 g (95%) of **14a** as a colorless oil: R_f 0.38 (silica gel, AcOEt/hexane 3:1); $[\alpha]^{20}_D = -12.9$ (*c* 1.0, CH_2Cl_2); IR (film) ν 3276 (NH), 2981, 2935 (CH), 1745, 1714 (C═O), 1250 (CO), 1167 (P═O) cm^{-1}; ^1H NMR ($CDCl_3$) δ 1.13 (d, $J = 6.9$ Hz, 3H), 1.23−1.35 (m, 9H), 1.44 (s, 9H), 1.61 (ddd, $J = 18.2$, 15.3, 10.1 Hz, 1H), 1.86 (ddd, $J = 20.6$, 15.3, 2.9 Hz, 1H), 2.32−2.46 (m, 1H), 4.06−4.24 (m, 7H), 5.40 (brd, $J = 8.0$ Hz, 1H); ^{13}C NMR ($CDCl_3$) δ 14.2 (CH_3), 16.4 ($J = 5.9$ Hz, CH_3), 17.4 (CH_3), 28.3 (CH_3), 28.6 ($J = 141.4$ Hz, CH_2), 31.9 (CH), 58.6 ($J = 16.0$ Hz, CH), 61.4 (CH_2), 61.5 ($J = 6.4$ Hz, $POCH_2$), 61.7 ($J = 6.4$ Hz, $POCH_2$), 79.9 (C), 155.3 (CO), 171.0 (CO); ^{31}P NMR ($CDCl_3$) δ 30.92; FABMS *m*/*z* 382 (MH^+, 36), 326 ($[M - C_4H_8]H^+$, 29), 282 ($[M - C_5H_9O_2]H^+$, 100).

Ethyl (2*R*,3*R*)-2-[*N*-(*tert*-Butoxycarbonyl)amino]-4-diethoxyphosphoryl-3-methylbutanoate (14b). Prepared following the same procedure as described above for **14a**, starting from 1.0 g of amino ester (−)-**12b**. Purification by flash chromatography (silica gel, AcOEt/hexane 3:1 to AcOEt) afforded 1.29 g (96%) of **14b** as a colorless oil: R_f 0.38 (silica gel, AcOEt/hexane 3:1); $[\alpha]^{20}_D = -20.2$ (*c* 0.9, CH_2Cl_2); IR (film) ν 3265 (NH), 2980, 2935 (CH), 1745, 1714 (C═O), 1250 (C═O), 1164 (P═O) cm^{-1}; ^1H NMR ($CDCl_3$) δ 1.02 (d, $J = 6.9$ Hz, 3H), 1.27−1.35 (m, 9H), 1.44 (s, 9H), 1.58 (ddd, $J = 17.3$, 15.5, 9.6 Hz, 1H), 2.00 (ddd, $J = 19.5$, 15.5, 3.8 Hz, 1H), 2.50−2.60 (m, 1H), 4.05−4.24 (m, 6H), 4.37 (brd, 1H), 5.20 (brd, $J = 8.1$ Hz, 1H); ^{13}C NMR ($CDCl_3$) δ 14.2 (CH_3), 15.8 ($J = 4.8$ Hz, CH_3), 16.4 ($J = 6.0$ Hz, CH_3), 28.3 (CH_3), 29.3 ($J = 141.0$ Hz, CH_2), 31.4 ($J = 2.3$ Hz, CH), 58.2 ($J = 15.9$ Hz, CH), 61.4 (OCH_2), 61.5 ($J = 6.8$ Hz, $POCH_2$), 61.6 ($J = 6.8$ Hz, $POCH_2$), 79.9 (C), 155.7 (CO), 171.3 (CO); ^{31}P NMR ($CDCl_3$) δ 31.17; FABMS *m*/*z* 382 (MH^+, 17), 326 ($[M - C_4H_8]H^+$, 10), 282 ($[M - C_5H_9O_2]H^+$, 100).

(4*S*,5*R*)-5-[*N*-(*tert*-Butoxycarbonyl)amino]-2-ethoxy-4-methyl-2-oxo-1,2-oxaphosphorinane (15a). Over a cooled suspension (0 °C) of $LiBH_4$ (214 mg, 9.83 mmol) in 70 mL of dry THF was added dropwise a solution of **14a** (2.5 g, 6.56 mmoL) in 20 mL of THF, and the resulting mixture was stirred for 16 h at room temperature. Then, the reaction mixture was cooled to 0 °C, and HCl 2 N was added to reach pH = 7. THF was evaporated and the aqueous phase extracted with AcOEt, dried (Na_2SO_4), and evaporated. The crude material was purified by flash chromatography (silica gel, AcOEt/hexane 3:1 to AcOEt) to give 1.41 g (73%) of **15a** as a colorless solid: mp (AcOEt) 121−124 °C; R_f 0.34 (silica gel, AcOEt/hexane 3:1); $[\alpha]^{20}_D = +74.8$ (*c* 1.0, CH_2Cl_2); IR (KBr) ν 3285 (NH), 1701 (C═O), 1279 (P═O) cm^{-1}; ^1H NMR ($CDCl_3$) δ 1.05 (dd, $J = 6.7$, 3.4 Hz, 3H, $CHCH_3$), 1.36 (t, $J = 7.1$ Hz, 3H, OCH_2CH_3), 1.44 (s, 9H, $C(CH_3)_3$), 1.65 (ddd, $J = 15.4$, 13.1 Hz, 1H, H-3), 1.85 (ddd, $J = 19.1$, 15.4, 4.1 Hz, 1H, H-3), 2.22−2.37 (m, 1H, H-4), 3.80 (brd, $J = 9.4$ Hz, 1H, H-5), 4.08−4.23 (m, 4H, OCH_2), 5.20 (brd, $J = 9.4$ Hz, 1H, NH); ^{13}C NMR ($CDCl_3$) δ 16.4 ($J = 5.8$ Hz, OCH_2CH_3), 19.7 ($J = 18.8$ Hz, $CHCH_3$), 26.4 ($J = 125.9$ Hz, C-3), 28.3 ($C(CH_3)_3$), 33.4 ($J = 6.5$ Hz, C-4), 49.5 ($J = 4.1$ Hz, C-5), 61.1 ($J = 6.5$ Hz, $POCH_2$), 72.7 ($J = 6.8$ Hz, C-6), 77.0 ($C(CH_3)_3$) 155.3 (CO); ^{31}P NMR ($CDCl_3$) δ 23.35; FABMS *m*/*z* 294 (MH^+, 15), 238 ($[M - C_4H_8]H^+$, 60), 194 ($[M - C_5H_9O_2]H^+$, 100).

(4*R*,5*R*)-5-[*N*-(*tert*-Butoxycarbonyl)amino]-2-ethoxy-4-methyl-2-oxo-1,2-oxaphosphorinane (15b) was prepared following the same procedure as described above for **15a**, starting from 1.1 g of *N*-Boc-amino ester **14b**, to yield 621 mg (73%) of a colorless oil (2 diastereoisomers, 2.7:1): R_f 0.35 (silica gel, AcOEt/hexane 3:1); IR (film) ν 3260 (NH), 1713 (C═O), 1271 (P═O) cm^{-1}; ^1H NMR ($CDCl_3$) δ (signals for major diastereoisomer): 1.12 (dd, $J = 6.5$, 3.5 Hz, 3H), 1.35 (t, 7.1 Hz, 3H), 1.44 (s, 9H), 1.56−1.69 (m, 1H), 1.98−2.08 (m, 2H), 3.45−3.59 (m, 1H), 3.76 (dt, $J = 10.7$, 3.8 Hz, 1H), 4.10−4.31 (m, 3H), 4.40 (brd, 1H); ^{31}P NMR ($CDCl_3$) δ 23.95 (major), 25.78 (minor); FABMS *m*/*z* 294 (MH^+, 14), 238 ($[M - C_4H_8]H^+$, 60), 194 ($[M - C_5H_9O_2]H^+$, 100).

(4*S*,5*R*)-5-Amino-2-hydroxy-4-methyl-2-oxo-1,2-oxaphosphorinane (13a). BrTMS (0.32 mL, 2.45 mmol) was added dropwise over a cooled (0 °C) solution of **15a** (300 mg, 1.02 mmol) in 6 mL of dry CH_2Cl_2, and the mixture was stirred for 12 h. The reaction was quenched with MeOH, and the solvent was removed in vacuo. The crude material was purified by reversed-phase flash chromatography eluting with water to give 204 mg (82%) of HBr·**13a** as a colorless solid: R_f 0.90 (RP-18, H_2O); $[\alpha]^{20}_D = +35.6$ (*c* 1.2, H_2O); IR (film) ν 2906 (NH_3^+), 1262 (P═O), 969 (POH) cm^{-1}; ^1H NMR (400 MHz, D_2O) δ 1.16 (dd, $J = 7.4$, 2.9 Hz, 3H, CH_3), 1.61 (dt, $J = 15.3$, 13.6 Hz, 1H, H-3), 1.87 (ddd, $J = 18.0$, 15.3, 4.4 Hz, 1H, H-3), 2.48−2.60 (m, 1H, H-4), 3.48−3.52 (m, 1H, H-5), 4.25 (ddd, $J = 20.6$, 13.6, 2.2 Hz, 1H, H-6), 4.23 (ddd, $J = 13.6$, 5.1, 2.2 Hz, 1H, H-6); ^{13}C NMR (DMSO-d_6) δ 18.9 ($J = 16.0$ Hz, CH_3), 26.7 ($J = 123.0$ Hz, C-3), 30.7 ($J = 6.1$ Hz, C-4), 50.1 ($J = 4.3$ Hz, C-5), 67.9 ($J = 5.8$ Hz, C-6); ^{31}P NMR ($CDCl_3$) δ 20.73; FABMS *m*/*z* 166 (MH^+, 100).

(4*R*,5*R*)-5-Amino-2-hydroxy-4-methyl-2-oxo-1,2-oxaphosphorinane (13b). Prepared following the same procedure as described above for **13a**, starting from 300 mg of *N*-Boc-amino ester **15b** to yield 211 mg (84%) of a colorless solid: mp > 200 °C (dec); R_f 0.90 (RP-18, H_2O); $[\alpha]^{20}_D = +7.6$ (*c* 0.95, H_2O); IR (KBr) ν 3035 (NH_3^+), 1256, 1236 (P═O), 991 (POH) cm^{-1}; ^1H NMR (400 MHz, D_2O) δ 1.20 (dd, $J = 7.4$, 2.2 Hz, 3H, CH_3), 1.61 (dt, $J = 10.8$, 15.1 Hz, 1H, H-3ax), 1.97 (ddd, $J = 17.0$, 15.1, 4.0 Hz, 1H, H-3ec), 2.22−2.38 (m, 1H, H-4), 3.24 (dt, $J = 3.2$, 9.1 Hz, 1H, H-5), 4.10 (dt, $J = 15.4$, 9.1 Hz, 1H, H-6ax), 4.35 (ddd, $J = 15.4$, 11.8, 3.2 Hz, 1H, H-6ec); ^{13}C NMR (DMSO-d_6) δ 19.1 ($J = 14.2$ Hz, CH_3), 28.2 ($J = 124.9$ Hz, C-3), 31.7 ($J = 6.2$ Hz, C-4), 51.3 ($J = 4.8$ Hz, C-5), 65.7 ($J = 5.6$ Hz, C-6); ^{31}P NMR ($CDCl_3$) δ 21.44; FABMS *m*/*z* 166 (MH^+, 100).

Acknowledgment. M.R. and V.O. thank the European Union (COMMET program) and Xunta de Galicia (XUGA 10306A98) for the grants awarded.

Supporting Information Available: ^{13}C NMR spectra for compounds **10a**,**b**, **12a**,**b**, **6a**,**b**, **14b**, **15a**, and **13b**, as well as *Z*-matrixes and heat of formation of the PM3-optimized structures. This material is available free of charge via the Internet at http://pubs.acs.org.

JO991402W